Supporting Information

Chitosan-α-Naphthaldehyde Hydrogel Film containing Pineapple Leaf Fiber for Wound Dressing Application

Amarjyoti Mondal[a], Dasuklang Lyngdoh Nongbri[b], Kusumita Achariya[c], Mahabul Haque[a],

Kripmoy Aguan[b], Arijit Bhattacharya[c], Atanu Singha Roy[a],*

[a] Department of Chemical and Biological Sciences, National Institute of Technology Meghalaya, Shillong-793003, India

[b] Department of Biotechnology & Bioinformatics, North-Eastern Hill University, Shillong 793022, India

[c] Department of Microbiology, School of Life Science and Biotechnology, Adamas University, Kolkata-700126, India

*Corresponding Author: Atanu Singha Roy
Tel.: +91 364 2501294
Fax: +91 364 2501113
Email: singharoyatanu@gmail.com; asroy86@nitm.ac.in

Experimental Section

1.1 Powder X-ray diffraction (PXRD)

The Powder X-ray diffraction (PXRD) pattern of the sample was recorded using an X-ray diffractometer (Rigaku Smartlab SE, Rigaku Corporation, Japan) equipped with Cu Kα characteristic radiation (wavelength λ = 1.5406 nm), which is operated at a voltage of 40 kV and a current of 50 mA. The data collection scanning rate was set at 2 degrees per minute, and 2θ angles covered from 5 to 50°. The crystallinity index of the chitosan and the prepared hydrogel film was calculated using the following Equation (Eqn S1).

$$Cryatallinity\ Index\ (CI) = (\frac{Area\ of\ the\ crystalline\ peak}{Area\ of\ the\ all\ peaks\ (crystalline + amorps)})$$

(S1)

1.2 Fourier-transform infrared (FT-IR) spectroscopy study

The FTIR spectra of chitosan, α-Naphthaldehyde, and the prepared hydrogel were recorded in the range of 400 cm^{-1} to 4000 cm^{-1} using an FTIR spectrophotometer (PerkinElmer Spectrum Two instrument) equipped with UATR accessories (0.5 cm^{-1} resolution).

1.3 FESEM (Field Emission Electron Microscopy)

Using the ZEISS Gemini 360 instrument, the hydrogel film's texture and surface roughness were measured in the in-lens mode at a 5 KV acceleration voltage. Before taking the image, we coated the sample with Au-Pd coating prior to image capture.

1.4 SEM (Scanning Electron Microscopy)

The surface morphology and texture of hydrogel film after the biodegradation test were taken using the SEM (JSM-6360 (JEOL)], which is accelerated from 1KV-30KV in the 1KV step. Before taking the image, we coated the sample with Au coating prior to image capture.

1.5 Mechanical Testing

The tensile strength of the hydrogel film was determined using a universal testing machine (UTM) [ASTM D638]. During the measurement of tensile strength, a 1.0 KN load cell and a crosshead speed of 5 mm/min were employed.

1.6 Cytotoxicity studies of the PLF-hydrogel film.

The MTT assay is known for its safety and sensitivity and is a widely used *in vitro* test to assess cell viability. This colorimetric assay measures the reduction of the tetrazolium dye MTT (3-[4,5-dimethylthiazol-2-yl]-2,5-diphenyltetrazolium bromide) into purple formazan crystals by metabolically of active cells. The intensity of the resulting purple color, measured spectrophotometrically, is directly proportional to the number of viable cells. For the assay, freshly cultured HEK-293 cells were diluted in an Advanced MEM culture medium (Gibco, ThermoFisher) to a concentration of 1×10^3 cells mL^{-1}. Then, 100 µL of this cell suspension was added to each well of a 96-well plate in triplicate and incubated for 24 hours at 37°C in a 5% CO_2 environment. After this initial incubation, the medium was replaced with 100 µL of fresh DMEM (low glucose without phenol, Himedia) containing different concentrations of PLF-Hydrogel film (4,6,8 and 10 mg/mL). The cells were then incubated for an additional 24 hours under the same conditions. Following the second incubation, 10 µL of MTT reagent was added to each well, and the plate was wrapped in aluminium foil to protect it from light. The plate was incubated for another 4 hours. To dissolve the formazan crystals, 100 µL of solubilization solution was added to each well, and the plate was shaken for 30 minutes. The absorbance at 570 nm was measured using a 96-well plate reader (Synergy H1 Hybrid reader, BioTek). Cell viability was then calculated based on the absorbance readings using the following formula (Eqn S2).

$$\% \, Cell \, viability = \frac{Absorbance \, of \, the \, treated \, cell \, (with \, PLF - Hydrogel \, film)}{Absorbance \, of \, the \, control}$$

(S2)

An automated inverted research microscope (Leica DMI4000 B) was used to take the images.
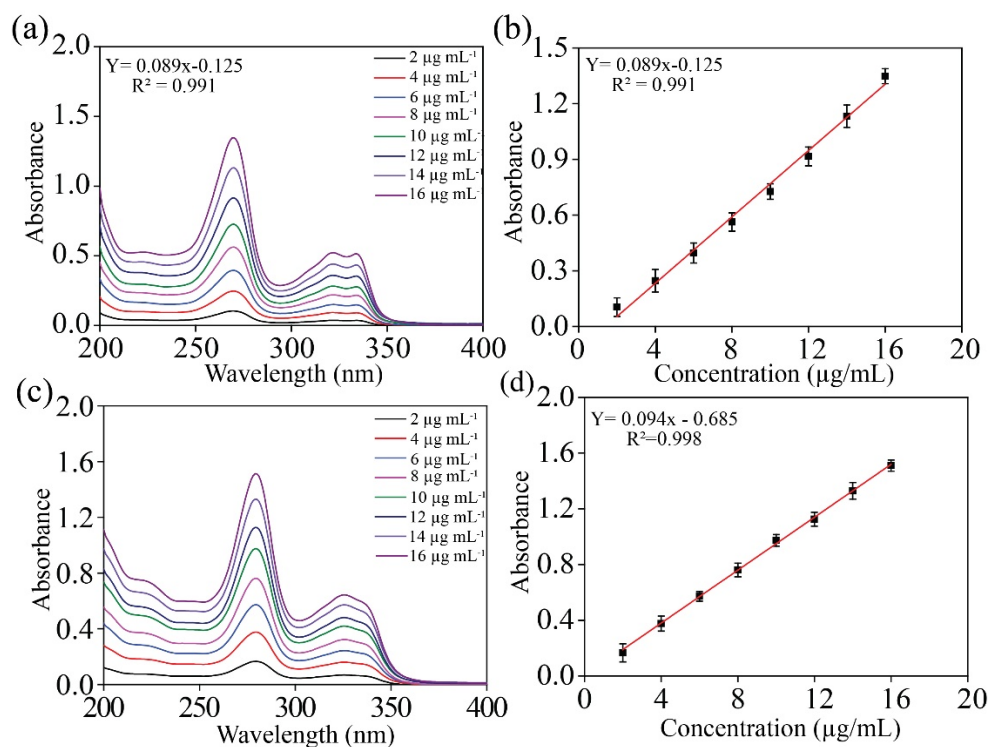
Figure S1. UV-Vis spectra of (a) lomefloxacin at 280 nm and (b) calibration curve of lomefloxacin, (c) UV-Vis spectra of ciprofloxacin at 270 nm and (d) calibration curve of ciprofloxacin.
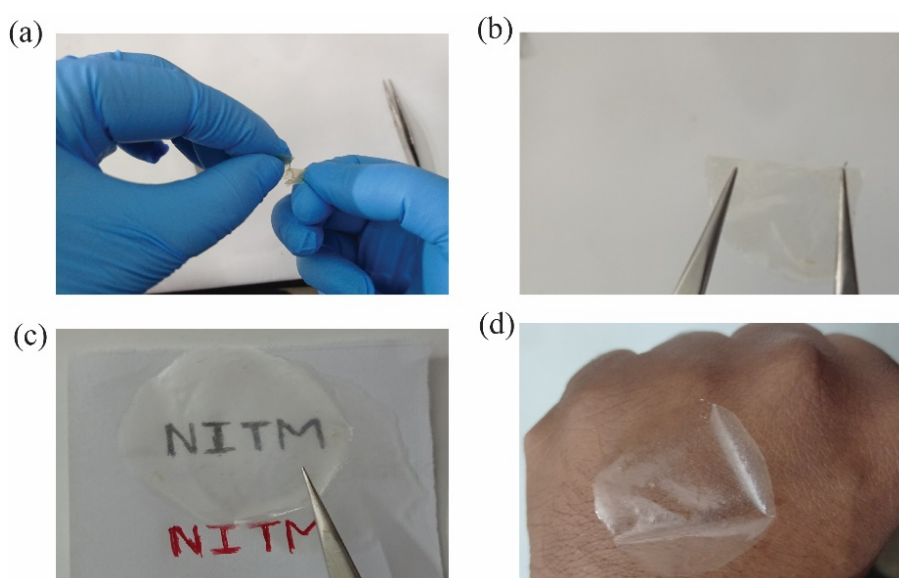

Figure S2. (a) Bending, (b) stretching with forceps, and (d and e) visual inspection of the NITM and skin through the hydrogel film.
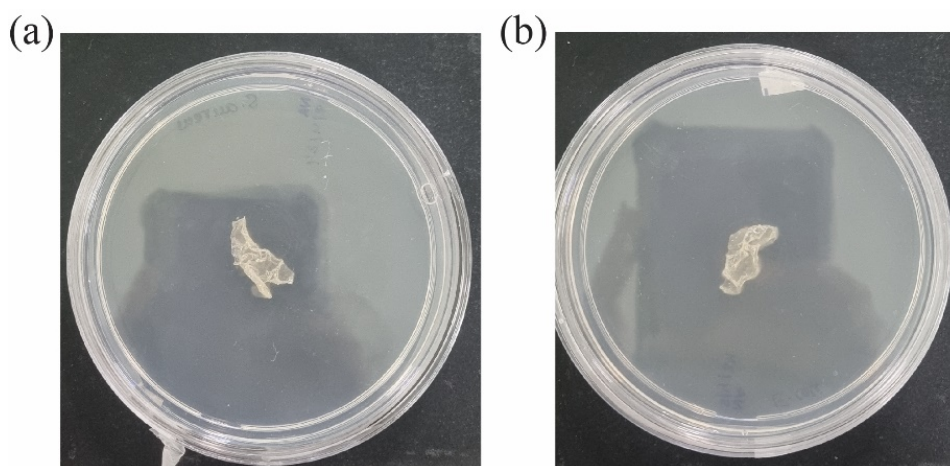
Figure S3. Digital photograph of the microbe penetration test of the hydrogel film in () E.coli (b) S.aureus bacterial strains for 5 days.
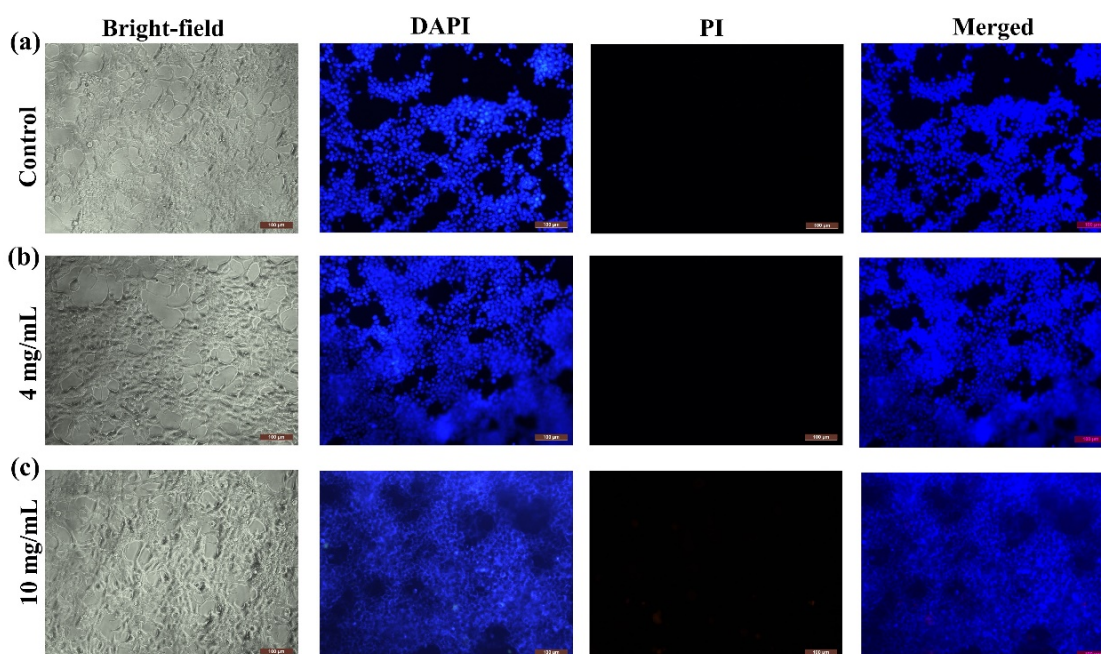

Figure S4. Fluorescence microscope (Leica DMI4000 B) images of (a) untreated HEK 293 cells (control), (b) 4 mg/mL, and (c) 10 mg/mL treated HEK 293 cells with PLF-Hydrogel films (scale bar 100 μm).

Table S1: The most significant peaks of the hydrogel from FT-IR

Sample	ν_{C-N}	$\nu_{C=N}$ (imine)	$\nu_{(bridge\ C-O-C)}$	$\nu_{C=C}$ (aromatic)	ν_{C-H} (aromatic)
Aldehyde	absent	absent	absent	absent	absent
Chitosan	1417	absent	1150	absent	absent
Hydrogel	1049	1647	1046	absent	728

Table S2: PXRD data of Cs (Chitosan) and the hydrogel film.

Sample	2θ	Crystallinity index (%)
Chitosan	10.52 and 19.93	97.10
Hydrofilm	22.30	66.25

Table S3: Different kinetics parameters of the release of ciprofloxacin from the gel network.

Drug release systems	Korsmeyer and Peppas power law		Zero order R^2	Pseudo-first order R^2	Higuchi square root law R^2
Hydrogel Film	n	R^2	0.962	0.950	0.950
	0.857	0.984			

Table S4: Different kinetics parameters of the release of lomefloxacin from the gel network.

Drug release systems	Korsmeyer and Peppas power law		Zero order R^2	Pseudo-first order R^2	Higuchi square root law R^2
Hydrogel Film	n	R^2	0.989	0.943	0.960
	0.828	0.943			

Table S5. Comparison of the application of different types of chitosan-based hydrogel with their applications.

Hydrogel name	Primary materials	Crosslinking method	Application	References
Cat-CH/ Hydrogel	Sodium bicarbonate, chitosan、EDC	physical crosslinking	Injectable Adhesion Carriers	2
OS Chitosanbased Hydrogel	Chitosan, tapioca starch, sodium periodate	Physical crosslinking	Drug delivery vehicles	3
SG/CS Hydrogel	Succinoglycan (SG), chitosan, 5-fluorouracil	Physical crosslinking	Ph Responds to Changes in Drug Delivery Systems	4
Dual-crosslinked CMC-ALG hydrogels	Carboxymethyl chitosan, alginate, calcium chloride, EGF powder	Physical crosslinking	Clinical Wound Care Wound Aids	5
TEPA – COS hydrogel	Tetraacetylethylenediamine (TEPA), epichlorohydrin (ECH), low chitosan	Physical crosslinking	As flexible sensors, wearable devices, and energy harvesting devices	6
(Fe^{3+}PCS/CSfHNTs NC hydrogel)	Acrylamide (AAm), acrylic acid (AAc), ammonium persulfate (APS), kaolin nanotubes (HNTs), hyperbranched polysiloxane (HSiv)	Physical crosslinking	For load-bearing structural materials	7
CS-TPP-hydrogel	Chitosan, tripolyphosphate (TPP), SQR22 dye, dimethyl sulfoxide (DMSO)	Physical crosslinking	Drug delivery	8
Chitosan Hydrogel modified cotton fabrics	Chitosan polymer, amylase, sodium bisulfite ($Na_2S_2O_4$),	Physical crosslinking	Significant antimicrobial activity, pH sensitivity, good mechanical	

	monochloroacetic acid (CAA), sodium carbonate (Na2CO3), reactive dye (Supra rouge SPX)		properties	9
Chitosan-α-Napthaldehyde Hydrogel film	Chitosan, α-Naphthaldehyde	Physical Crosslinking (Covalent Crosslinking)	pH-responsive swelling behavior, Antibiotics delivery, High Encapsulation Efficiency, Water Vapour Transmission Rate (WVTR), Drug release kinetics, Microbe Penetration, Biodegradation	**Present Work**
PLF-Hydrogel film	Chitosan, α-Naphthaldehyde, and PLF	Physical Crosslinking (Covalent Crosslinking) infusion with PLF	pH-responsive swelling behavior, High mechanical strength, Reatin its mechanical strength after swelling, Cell viability (against HEK-293), Antibacterial activity	**Present Work**

References.

2 C. Guyot, M. Cerruti and S. Lerouge, *Mater. Sci. Eng. C*, 2021, **118**, 111529.

3 D. Sarmah, M. A. Rather, A. Sarkar, M. Mandal, K. Sankaranarayanan and N. Karak, *Int. J. Biol. Macromol.*, 2023, **237**, 124206.

4 J. Kim, Y. Kim, J. Jeong, J.-M. Kim, M. S. Kim and S. Jung, *Int. J. Biol. Macromol.*, 2023, **242**, 124888.

5 Y. Hu, Z. Zhang, Y. Li, X. Ding, D. Li, C. Shen, F.-J. Xu, *Macromol. Rapid Commun.*, 2018, **39**, e1800069.

6 F. Hong, P. Qiu, Y. Wang, P. Ren, J. Liu, J. Zhao and D. Gou, *Food Chem. X*, 2024, **21**, 101095.

7 S. N. Li, B. Li, Z. R. Yu, Y. Li, K. Y. Guo, L. X. Gong, Y. Feng, D. Jia, Y. Zhou and L. C. Tang, *Compos. Part B Eng.*, 2020, **194**, 108046.

8 J. H. Lim, D. Kai, C. Lee, *New J. Chem.,* 2023, **47**, 550-553

9 M. Trad, W. Miled, S. Benltoufa, A. Boughattas, R. Benslama, F. Fayala and A. Bakhrouf, *J. Appl. Polym. Sci.*, 2018, **135**, 46645.